Construction and Building Materials 246 (2020) 118430

Contents lists available at ScienceDirect

Construction and Building Materials

journal homepage: www.elsevier.com/locate/conbuildmat

Behavior of geopolymer concrete under cyclic loading

Aslam Hutagi [a,*], R.B. Khadiranaikar [b], Aijaz Ahmad Zende [c]

[a] Associate Professor, Department of Civil Engineering, SECAB Institute of Engineering and Technology, (Affiliated to Visvesvaraya Technological University, Belagavi), Vijayapur, India
[b] Professor, Department of Civil Engineering, Basaveshwar Engineering College, (Government aided institution affiliated to Visvesvaraya Technological University, Belagavi) Bagalkot, India.
[c] Assistant Professor, Department of Civil Engineering, BLDEA's Vachana Pitamaha Dr P.G.Halakatti College of Engineering and Technology, (Affiliated to Visvesvaraya Technological University Belagavi), Vijayapura, India.

HIGHLIGHTS

- Behaviour of high strength GPC under repeated loading.
- Envelope curves under cyclic compressive loadings are studied.
- Locus of common and stability points is determined.
- Analytical equations are proposed for envelope, common and stability point curve.

ARTICLE INFO

Article history:
Received 24 March 2019
Received in revised form 14 January 2020
Accepted 12 February 2020

Keywords:
Geopolymer concrete
Stress-strain curve
Envelope curve and common point curve
Plastic Strain

ABSTRACT

Much effort has been done on compressive strength of Geo Polymer Concrete (GPC) under monotonic loading to study the mechanical and durability properties. It is also very important to study its behavior when the concrete members are subjected to cyclic loads. In this research, some new concepts of nature of stress-strain curve, envelope curve and common point curve of geopolymer concrete are presented for three different grades of GPC. Investigations related to study of stress-strain characteristics of geopolymer concrete under cyclic loading is focused. The locus of common and stability points was determined from the cyclic stress-strain curve. The identification of these is an important contribution for the design of GPC. Analytical equations were proposed for envelope curve, common point curve and stability point curve. The Proposed curves fit well with experimental test data.

1. Introduction

The earliest work on fatigue of mortar specimens in compression was carried out in 1898 and concrete specimen in 1903. The various models are available for determining the stress-strain hysteresis of confined concrete under monotonic loading [1–4]. Sinha et al. 1964 [5] and Karsan and Jisra 1969 [6] conducted uniaxial compressive tests on unconfined concrete specimens to evaluate unloading and reloading paths. Bahn, B.Y et al. [7] proposed a stress-strain model of concrete for cyclic loading based on a series of uniaxial loading tests on unconfined concrete.

Park et al. 1972 [8] and Mander et al. 1988 [9] proposed stress-strain models of confined concrete that included unloading and reloading paths. Park et al. simplified both unloading and reloading paths to be straight lines. They proposed using a fractional expression for unloading paths and a combination of a straight line and a quadratic function for reloading paths. However, a few researchers [10], pointed out that the quadratic function could not represent the reloading paths, and proposed using a cubic function instead of the quadratic function. Martinez-Rueda and Elnashai [11] modified the model proposed by Mander et al. to include the effect of degradation of strength and stiffness due to cyclic effects. Mendola and Papia, 2002 [12] proposed a unique model that is applicable for both concrete and masonry under cyclic loading.

Sakai and Kawashima, 2000 [13] and Sakai et al. 2000 [14] conducted a series of compressive loading tests on reinforced concrete column specimens to determine the repeated unloading/ reloading cycles including partial loading on the hysteretic behavior of confined concrete. Based on this research, they proposed an unloading and reloading stress-strain model for typical unloading and reloading paths, i.e., an unloading path from an envelope curve and a reloading path from zero stress. According to Sakai and Kawashima [13], a few stress-strain models have been proposed for unloading and reloading paths. Although these models predict the hysteretic behavior of confined concrete with certain degree of accuracy, they

* Corresponding author.
E-mail address: aslamhutagi_cv@secab.org (A. Hutagi).

https://doi.org/10.1016/j.conbuildmat.2020.118430
0950-0618/

do not include the effect of repeated unloading reloading excursions or partial loading. Therefore, a more advanced model that includes these parameters is needed for more accurate analyses.

R.B. Khadiranaikar and S.N. Sinha [15] did experimental investigation on high-performance concrete under uniaxial repeated compressive loading. The strength of high-performance concrete was 65, 85 and 102 MPa. The test was carried on the stress-strain relationships under repeated compressive loading, Envelope, common point, stability point and analytical expression is proposed for these curves, which was found to have reasonable fit with the experimental data. It was concluded that the peak stress of the stability point curve could be regarded as the maximum permissible stress. It was also observed that the permissible stress level depends on the plastic strain level present in the material due to repeated loading.

The advantages of GPC proved to be useless because of heat curing, which is difficult in the field and limit its usage to precast elements only. Thus, researchers carried out works on how to replace heat curing by other alternatives. Some efforts were then made to produce the fly ash based GPC, which was cured at ambient temperatures [16]. They first produced the concrete by replacing cement with fly ash, but to reduce cement content to 0% and achieve strength, they added GGBFS to produce strength of 55 MPa at ambient curing. Apart from strength properties, GPC also proved to have excellent durability properties, better than conventional concrete made using Ordinary Portland Cement (OPC) [17–19].

It can be seen from the past research that most of the works carried out in this area are limited to curing at high temperature whose application will be restricted to only precast elements. With the advancement in technology, now we have a choice of making the GPC to be cast in the field, which requires atmospheric curing. But recently numerous researches have been carried on ambient curing of geopolymer concrete [20–25]. Methods are also developed to reduce setting time of GPC [26]. Thus, due to the insufficient data available regarding the behaviour of high strength GPC under repeated loading, this research work shall fill the gaps in understanding the behaviour of high strength GPC under repeated loadings and may help the other researchers and engineers to widely use this material in structures subjected to repeated type of loadings.

2. Materials

Materials used to produce GPC are class F fly ash, GGBFS, sand, coarse aggregate, alkaline liquid and superplasticizer. Class F fly ash from Raichur Thermal Power Station, Karnataka, India is used in the present study as one of the source materials. Granulated Blast-Furnace Slag(GGBFS) was taken from Jindal Steel Work (JSW) Bellary, Karnataka, India is used in this research as replacement of fly ash up to 40%. Table 1 shows the chemical composition of Fly ash and GGBFS. Coarse aggregates taken for this research work were 12 mm downsize with specific gravity of 2.72. Fine aggregates in the form of river sand passing from 4.75 mm sieve with specific gravity of 2.6 were taken for this experimental work

Alkaline solution plays a major role in geopolymer. The most common alkaline liquid used in geopolymerisation is a combination of sodium hydroxide (NaOH) and sodium silicate (Na_2SiO_3), The second generation of superplasticizer called Master Glenium B-833 from BASF India Ltd. is used.

3. 3.Experimental programme

3.1. Instrumentation

500 kN Servo hydraulic actuator is fitted on loading frame of capacity 200 Ton as shown in Fig. 1. The Compressometer, Circumferential Extensometer and Load cell are used to record data in this research. Compressometer is needed for change in longitudinal displacement of specimen. This measures the displacement on opposite sides of the test specimen and the output is average of two reading. They are self-supporting on the specimen and can be mounted very easily as shown in Fig. 1. Circumferential Extensometer is used to measures the circumferential expansion of cylindrical sample subjected to compressive loading and it gives the lateral displacement of specimen by which Poisson's ratio can be determined and is shown in Fig. 1.

3.2. Mixing and curing

Pan mixer is used for mixing of geopolymer concrete. The constituents of the geopolymer are coarse aggregate, fine aggregate, fly ash, GGBFS and alkaline solution. The wet mixing usually continued for another four minutes. The polymerization process is usually accelerated in an elevated temperature than ambient. This study aimed to produce geopolymer concrete based on fly ash and GGBFS with improved engineering properties in ambient curing. Fig. 2 shows ambient curing of GPC specimens.

3.3. Mixture proportion:

The density of geopolymer concrete is 2400 kg/m^3, where total aggregate is 77% of the entire mass. The remaining mass is combination of alkaline solution and binder (geopolymer paste). Alkaline solution to binder ratio is taken between 0.3 and 0.5. Sodium silicate solution to sodium hydroxide solution ratio is 2.5. Table 2 shows the mix proportion of geopolymer concrete.

4. Results and evaluation

4.1. Stress-strain envelope curve

Many GPC mixtures were prepared to achieve cylindrical strength in the range of 40–60 MPa by varying different parameters like alkaline liquid, slag, molarity content and water to geopolymer binder ratio and finally three mixes were finalized. In order to assess the behavior of GPC, 3 type of testing are conducted as given in Table 3. The cyclic loads can affect the structures in two categories. In the first category, the cyclic load effect may be due to fatigue, which is caused by large number of loading cycles with low-stress levels and in the second category, incremental deformations take place with less number of cycles but with higher stress levels. The present investigation is based on the second category.

In Monotonic Uni-axial loading test, loading was done uniformly so as to reach ultimate capacity. In repeated compressive

Table 1
Chemical composition of fly ash and GGBFS.

Sample	SiO_2	Al_2O_3	Fe_2O_3	CaO	MgO	Na_2O	K_2O	SO_3	P_2O_5	TiO_2	Loss on ignition
Fly ash (wt.)	62.50	24.50	6.40	3.80	0.6	0.48	0.52	0.45	0.1	1	0.34
GGBFS (%)	34.5	15.8	0.72	37.95	4.6	0.2	0.43	5.12	0.025	0.43	0.29

Fig. 1. Instrumentation to test GPC specimens.

Fig. 2. Ambient curing of GPC specimens.

loading-1, load histories were controlled by monitoring strain in each cycle in ascending zone and releasing the loads in descending zone of the stress-strain curve when it is about to descend. After performing the test, the curve possesses locus of common points, i.e. "A" point where reloading curves of all cycle crosses the unloading curves of preceding cycles. In repeated compressive loading 2, unloading in each cycle was made at the time reloading curve crossed the initial unloading curve. This point where the intersection slowly descends and gets stabilizes at a lower bound and thus forms a closed hysteresis loop after all cycles. Figs. 3a–d and 4a–c shows the stress-strain curves to obtain common points and stability points after testing cylinder of M40, M50 and M60 grade of concrete.

Under cyclic loading, envelope stress-strain curve was obtained by superimposing the peak stress-strain of cyclic loading on peaks of monotonic loading curve. These peaks were then plotted by expressing stress and strain. Many researchers have reported that envelope does not actually coincide with the monotonic curve but a few researchers have shown that it does coincide and hence it is still a controversial topic. In our case, as can be seen from Fig. 3d, the envelope is almost near to the monotonic curve. The stress and strain coordinates were normalized with respect to peak stress and strain for peak strain respectively for all specimens. Fig. 5a–c shows the normalized envelope stress-strain curve for cyclic loads. The mean strain values obtained were 0.00299, 0.003 and 0.0031 with a SD of 1.9×10^{-4}, 6.01×10^{-5} and 5.29×10^{-5} for M40, M50 and M60 mixes. The mean Stress values obtained were 47.20, 56.98 and 63.63 MPa with a SD of 1.9, 2.8 and 2 MPa for M40, M50 and M60 mixes.

Common Point curve: After carrying out the cyclic loading on specimen, a locus of common point was obtained, where reloading curves of all cycles crosses the unloading curves of proceeding cycle. These points are shown in Fig. 3d.

4.2. Analytical curves

From the test result data under cyclic loading, an expression was obtained for all the three curves of all mixes M1, M2 and M3 using MATLAB. The stress coordinates σ are normalized with regard to peak stress (f_m) for all specimens. The strain coordinates, ε, are normalized with regard to axial strain (e_m), when the peak stresses are achieved.

$$f(\sigma) = a_0 + a_1\cos(\varepsilon w) + b_1\sin(\varepsilon w) \quad (1)$$

where,

σ = Normalized stress-ratio, f/f_m
ε = Normalized strain ratios, e/e_m
f = stress
f_m = mean stress
e = strain
e_m = mean strain
I_c = coefficient of correlation,
a_0, a_1, b_1 and w = Equation constant

The above equation is in the form of a Fourier and the parameters obtained for the above equation for all the three curves of mixes M1, M2 and M3 are shown in Table 4.

Due to the fact that the microcracks initiate early in concrete with lesser strength, the mix M1 has a more stretched curve as compared to mix M2 or M3. The mix M1 has also larger plastic strain accumulation as compared to the other two mixes. Figs. 5a–c, 6a–c, 7, 8a–c shows analytical curves for all the 3 mixes. It can be seen from Table 4 that the coefficient of correlation, I_c, is almost more than 0.9 for envelope curves, common point curves and stability point curves which indicates a good fit for all the three mixes.

It can be inferred that; the envelope curve is similar for all the three mixes, for common point curves, peak stresses has a good comparison for all the three mixes and as the strength decreases, the stress ratio also decreases for stability point curve. Figs. 9a–c and 10a–c shows the combined analytical curves and repeated loading stress-strain curves.

4.3. Stability point curve

The stress and strain characteristics of Geopolymer concrete for uni-axial and bi-axial compressive monotonic loadings have been extensively studied by many researchers till date. However, the research on performance of high strength GPC under repeated loading condition is not much available. Understanding of cyclic behavior of high strength GPC is very important with regard to energy dissipation characteristics, materials ductility, and stiffness degradation. It has been reported that the strength decline is up to

Table 2
Mix proportion of geopolymer concrete.

Sl. No	Materials	40 MPa	M50 MPa	M60 MPa	Units
1	Unit Wt. of concrete	2400.00	2400.00	2400.00	Kg/m^3
2	Mass of aggregate	1848.00	1848.00	1848.00	Kg/m^3
	Coarse aggregate (12 mm)	1293.6	1293.6	1293.6	Kg/m^3
	Fine aggregate	554.40	554.40	554.40	Kg/m^3
3	Mass of binder and alkaline liquid	552.00	552.00	552.00	Kg/m^3
4	Alkaline liquid to binder ratio	0.40	0.35	0.3	
5	Mass of binder	394.28	408.88	424.61	Kg/m^3
	Fly ash	315.42 (80%)	286.21 (70%)	254.76 (60%)	Kg/m^3
	GGBFS	78.86 (20%)	122.66 (30%)	169.90 (20%)	Kg/m^3
6	Mass of alkaline liquid	157.72	143.12	127.39	Kg/m^3
7	Ratio of sodium silicate sol. to sodium hydroxide sol.	2.50	2.50	2.50	
8	Molarity	14	14	16	
9	Mass of sodium hydroxide sol.	45.06	40.89	36.52	Kg/m^3
10	Mass of sodium silicate sol.	112.66	102.23	91.28	Kg/m^3
11	In sodium silicate solution.				
	SiO_2 to Na_2O ratio	2.00	2.00	2.00	
	Na_2O	18.81	17.07	15.25	Kg/m^3
	SiO_2	39.88	36.19	32.31	Kg/m^3
	Water	53.96	48.96	43.72	Kg/m^3
12	In sodium hydroxide solution.				
	NaOH Solids	25.23	22.89	23.37	Kg/m^3
	Water	19.82	17.99	13.15	Kg/m^3
13	Water to geopolymer solids ratio by mass	0.24	0.22	0.20	
14	Amount of super plasticiser required	9.86 2.5%	12.27 3%	14.85 (3.5%)	Kg/m^3

Table 3
Type of Testing.

Sl No	Experiment	Description
1	Monotonic Uni-axial Loading test	Loading increased steadily till failure so as to obtain envelope stress-strain curve
2	Repeated Compressive loading-1 (Fig. 3a–d)	Keeping the peak Strain approximately similar to envelope curve to obtain common point.
3	Repeated compressive loading-2 (Fig. 4a–c)	Similar to that repeat compressive Loading-1, but loading and unloading were repeated more number of times to obtain stability point.

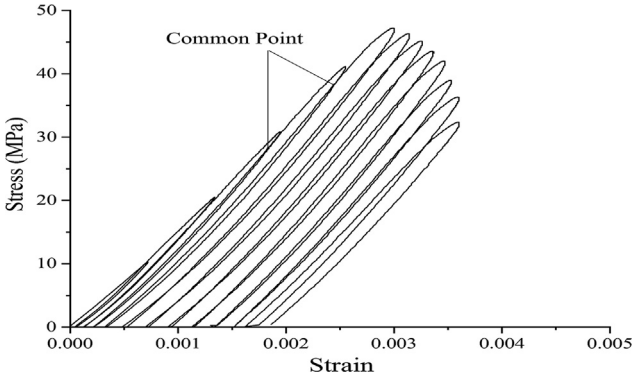

Fig. 3a. Common point test for M1.

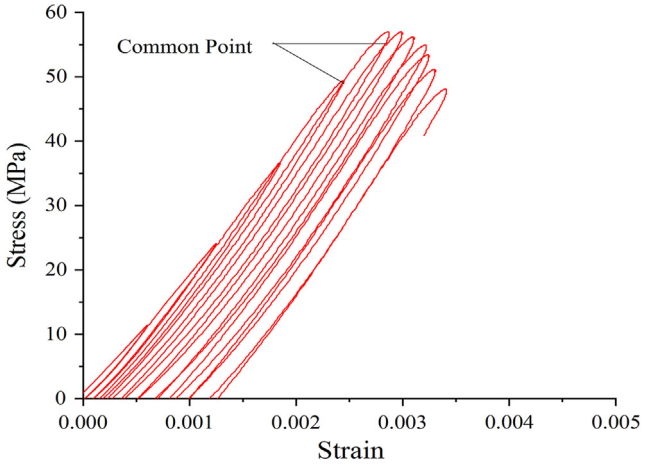

Fig. 3b. Common point test for M2.

30% due to repeated loading as compared to monotonic loading [27].

In the previous section, it was observed that the additional strains are produced when the stress reaches beyond the common point levels, whereas, loci of common points are formed in descending order when the stresses are under common point levels till they stabilize at the locus of stability point.

Stability point stress-strain curves are shown in Fig. 7 and stability points for the 3 mixes are shown in Fig. 8a–c. It is well known that the stability point curves of concrete when tested under repeated loading signify the permissible stress limits. The maximum permissible stresses can be obtained by these curves, i.e. peak stress of these curves. The permissible stress levels can also be obtained from plastic strains corresponding to stability-point peak stresses. Thus, the maximum permissible stress levels of GPC under repeated loadings are the peak stresses of these curves.

After performing tests, it produced 3 distinct stress-strain curves i.e., envelope, stability and common point. Cyclic loading −1, produced the locus of topmost points, i.e. a common point and Repeated compression loading-2, produced the locus of lowermost point i.e. stability point. Stresses above and below the common point produced additional strains and stress-strain path respectively.

Additional plastic strain to that of proceeding cycles was not observed when the load cycles with peak coincided with stability

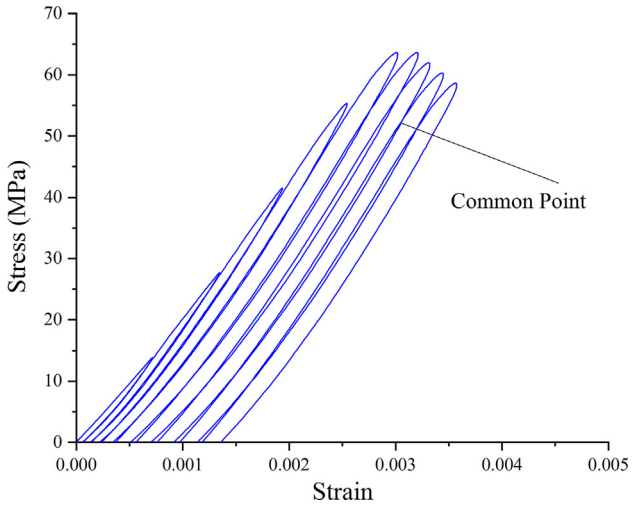

Fig. 3c. Common point test for M3.

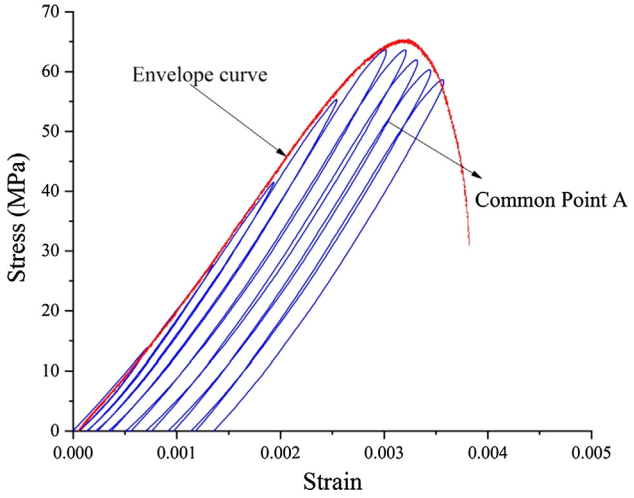

Fig. 3d. Envelope curve coincide with monotonic curve point.

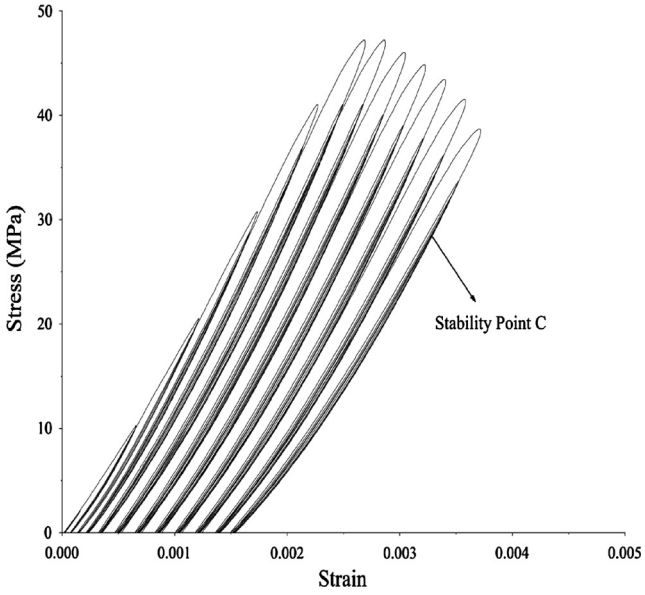

Fig. 4a. Stability point test for M1.

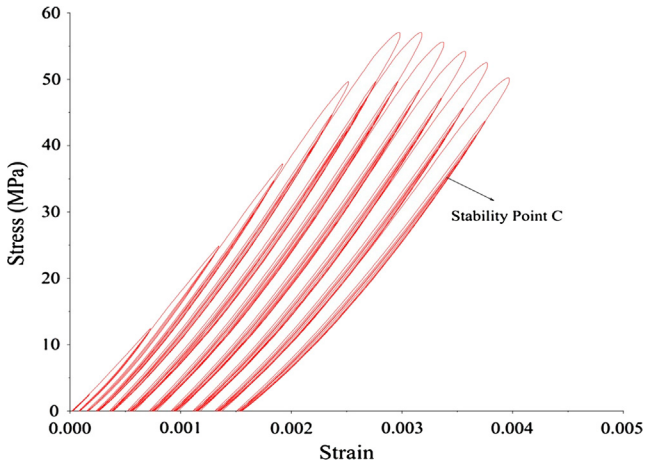

Fig. 4b. Stability point test for M2.

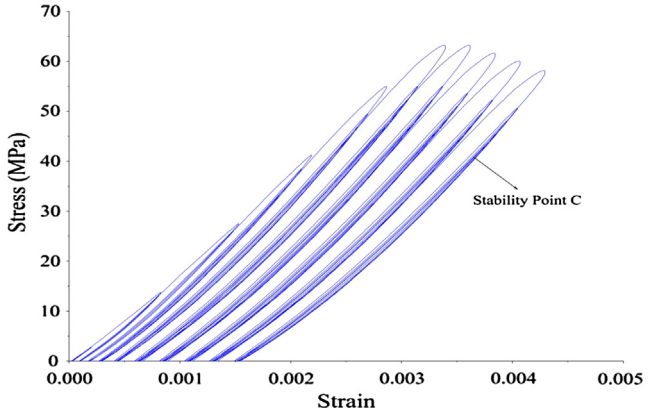

Fig. 4c. Stability point test for M3.

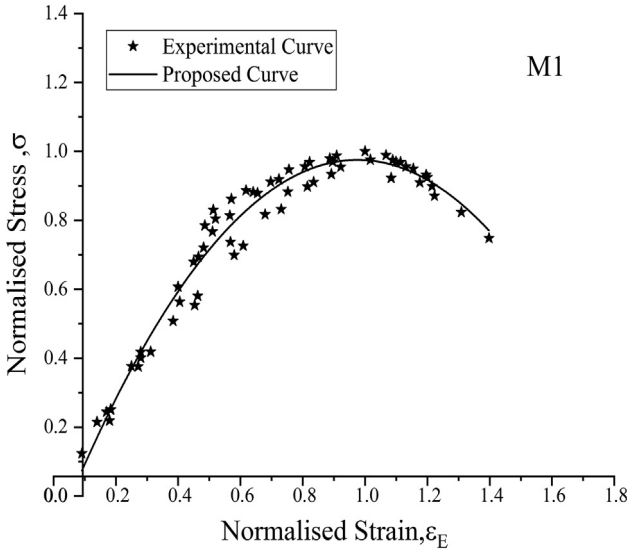

Fig. 5a. Normalized envelope stress-strain curve for M1.

point curve. But, when the load cycles exceed the stability point limits, continuous cycling will produce a number of plastic strains leading to failure. It was also observed that when the load cycles were well within the limits of stability point, continuous cyclic

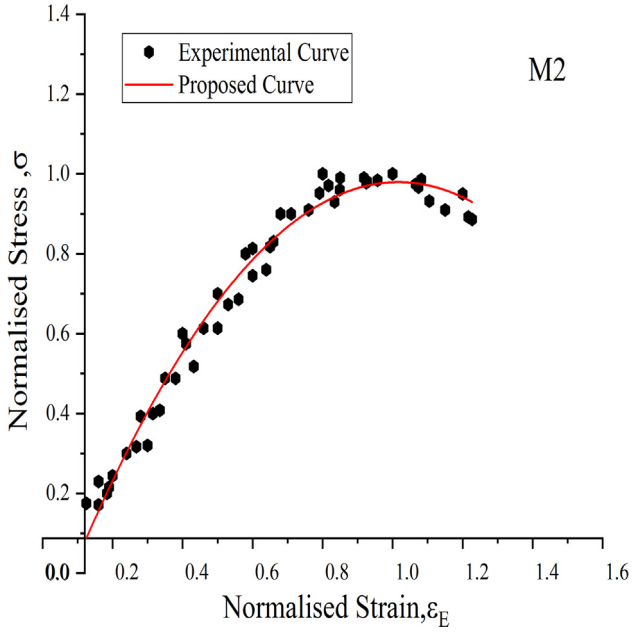

Fig. 5b. Normalized envelope stress-strain curve for M2.

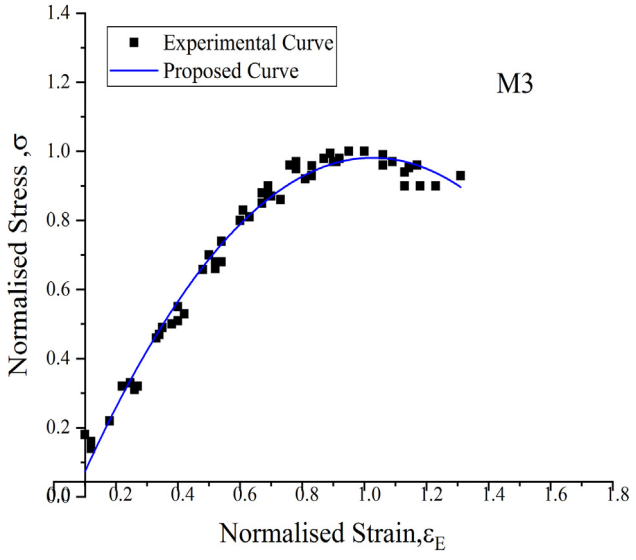

Fig. 5c. Normalized envelope stress-strain curve for M3.

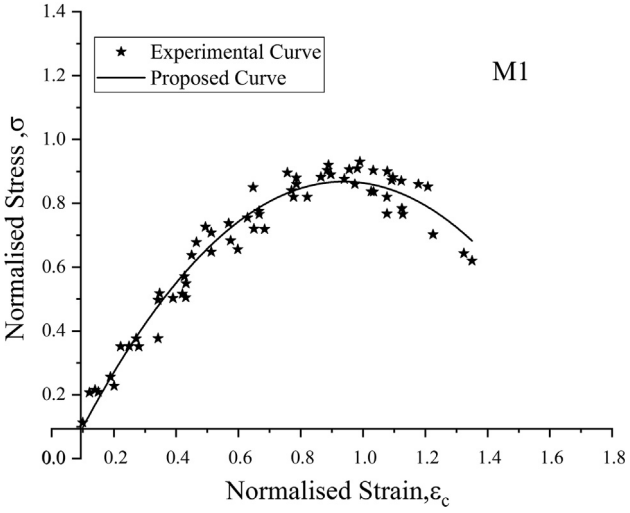

Fig. 6a. Common point stress-strain curve for M1.

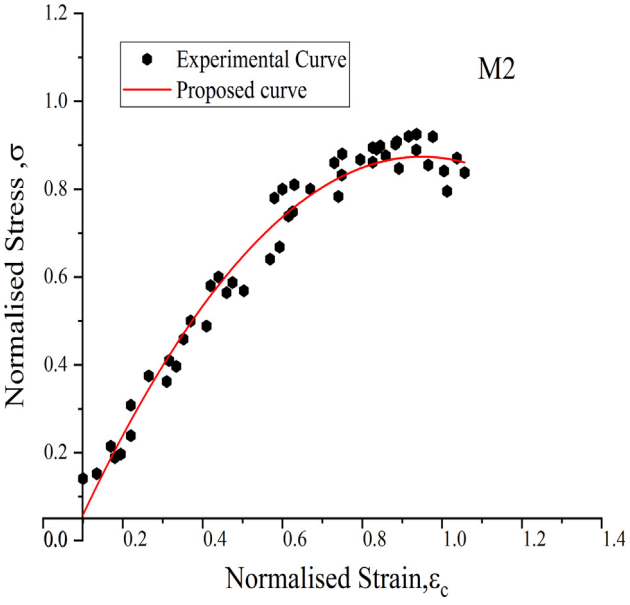

Fig. 6b. Common point stress-strain curve for M2.

Table 4
Values of $a_{0,}$ $a_{1,}$ $_{b1}$, w and Ic for envelope, common-points and stability point-curve.

Stress-strain curve	M1				
	a0	a1	b1	w	Ic
Envelope	−0.35	0.29	1.30	1.39	0.97
Common-point	0.30	−0.27	0.51	2.21	0.96
Stability-point	0.20	−0.19	0.49	2.49	0.96
	M2				
Envelope	0.42	−0.41	0.38	2.47	0.98
Common-point	0.4	−0.38	0.29	2.81	0.97
Stability-point	0.11	−0.13	0.62	2.07	0.95
	M3				
Envelope	0.36	−0.35	0.51	2.20	0.98
Common-point	0.40	0.37	0.31	2.64	0.96
Stability-point	0.31	−0.26	0.35	2.67	0.96

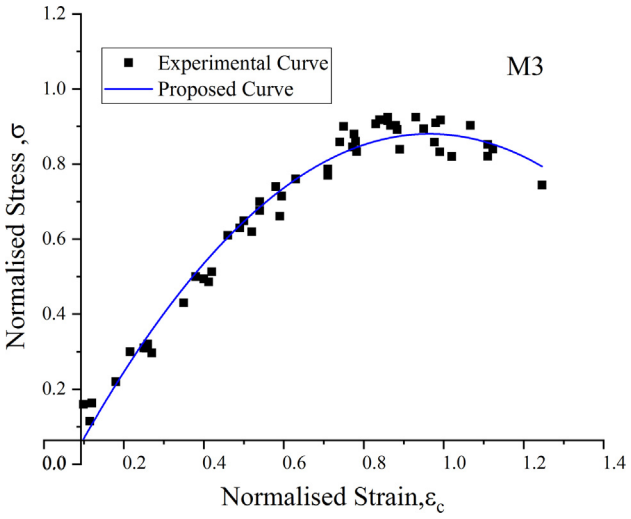

Fig. 6c. Common point stress-strain curve for M3.

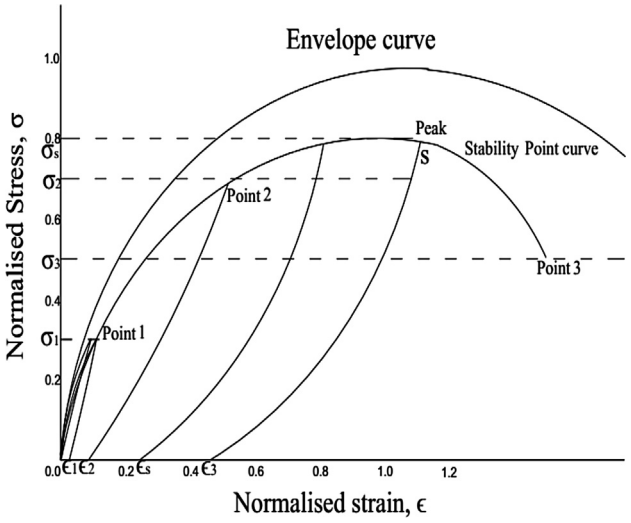

Fig. 7. Stability Point Stress-strain Curve.

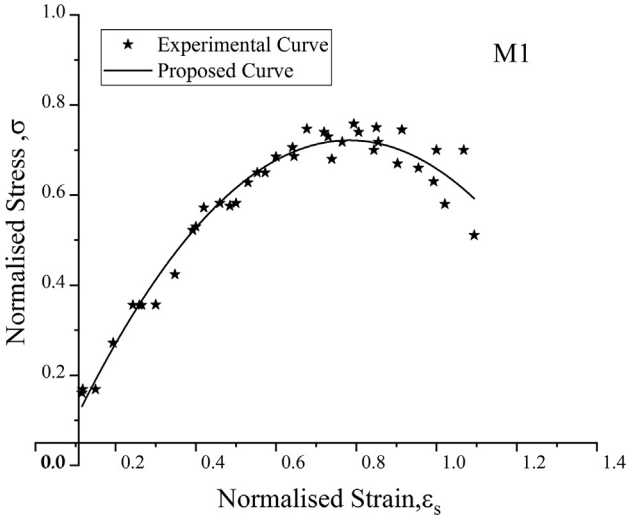

Fig. 8a. Stability Point Stress-strain Curve for M1.

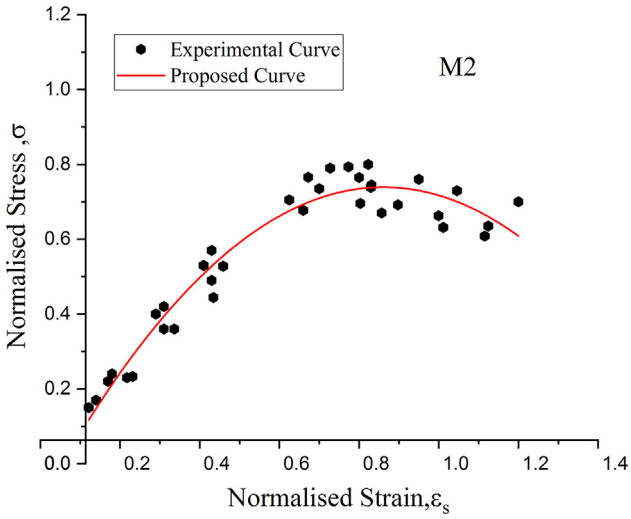

Fig. 8b. Stability Point Stress-strain Curve for M2.

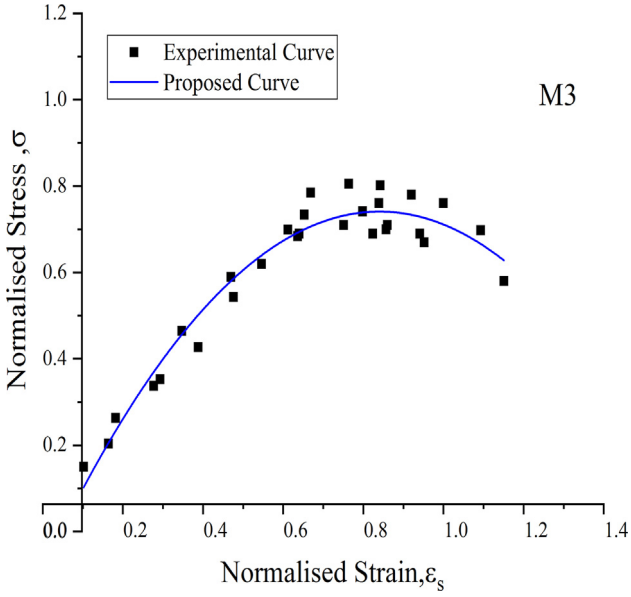

Fig. 8c. Stability Point Stress-strain Curve for M3.

produces plastic strains until the cycle coincides with stability point and further cycling stabilizes the plastic strain.

Thus, the level of plastic strains plays a vital role to determine permissible stress level. Hence, in this study the peak stress of stability point curve is considered as the maximum permissible stress level of GPC subjected to cyclic loading. This study provides a factor of safety of 1.2 whereas IS code [28] specifies value of 1.5. Fig. 9a–c shows the analytical curves for Envelope, common point and stability point curves for all the 3 mixes. Cyclic Normalised Stress-Strain curves of experimental and proposed Envelope, common point and stability point curves can be seen in Fig. 10a–c for all the 3 mixes.

4.4. Failure mode

GPC behaves similarly to that of normal concrete. In interfacial transition zone between paste matrix and aggregates, the microcracks cause a more brittle mode of fracture. It was found that

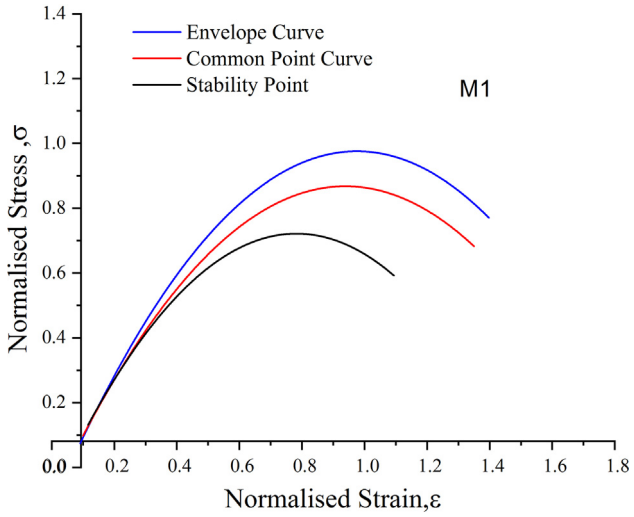

Fig. 9a. Analytical curves for M1 Mix.

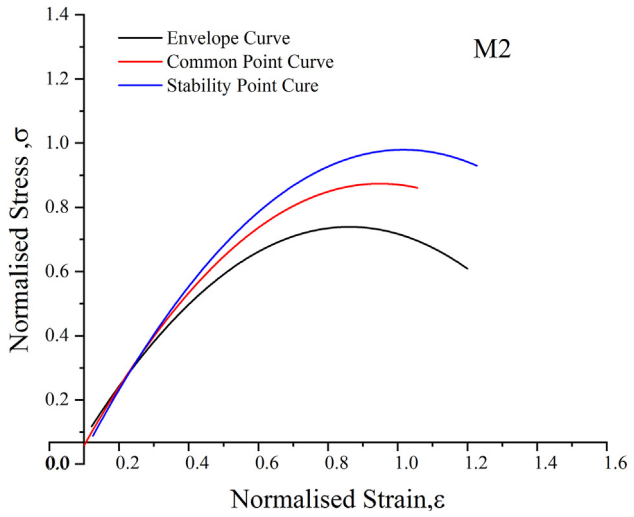

Fig. 9b. Analytical curves for M2 Mix.

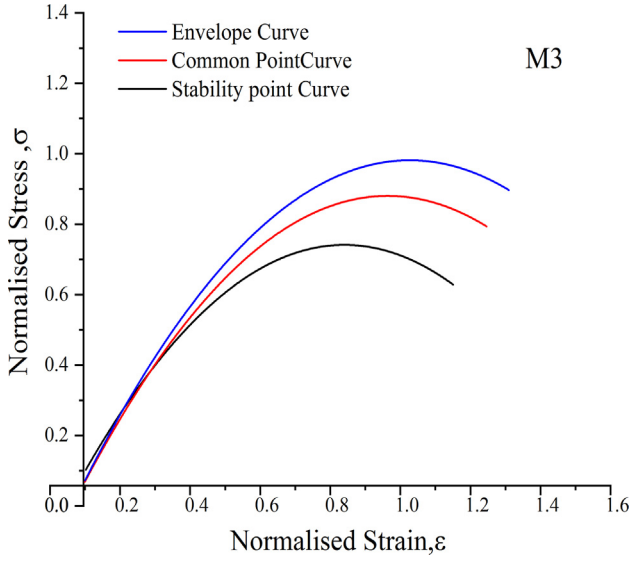

Fig. 9c. Analytical curves for M3 Mix.

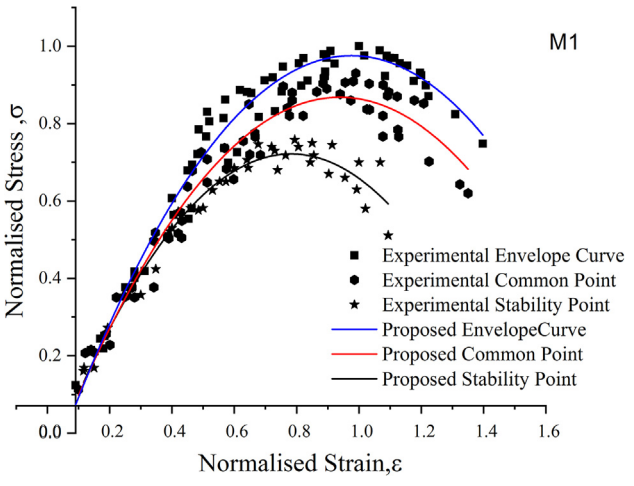

Fig. 10a. Cyclic Normalised Stress-Strain curves for M1 Mix.

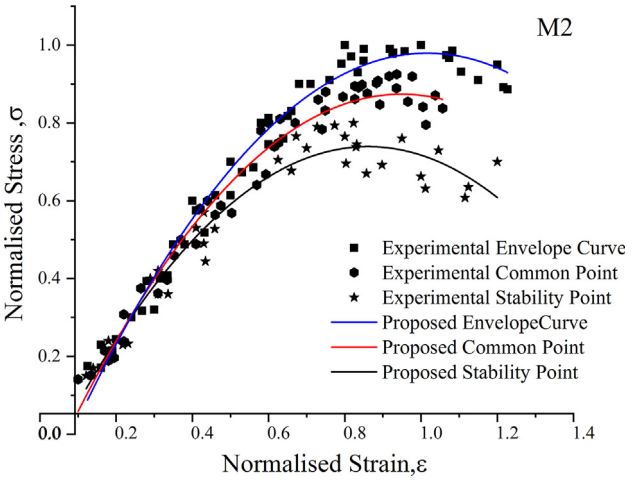

Fig. 10b. Cyclic Normalised Stress-Strain curves for M2 Mix.

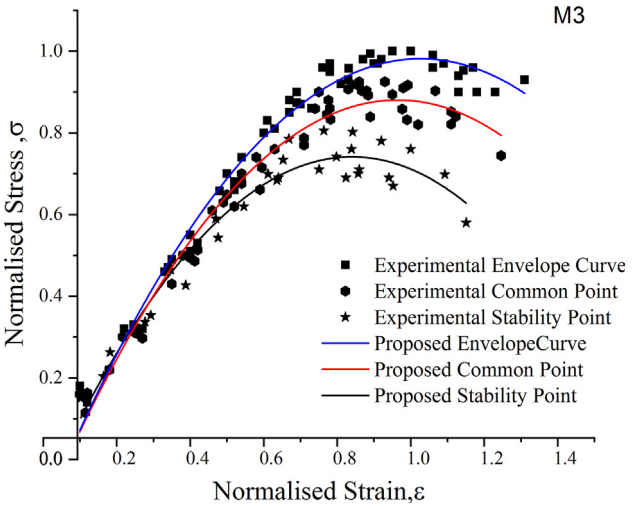

Fig. 10c. Cyclic Normalised Stress-Strain curves for M3 Mix.

cracks initiated at about 70–80 percent of peak local and started propagating towards the center. Failure took place by chipping of surfaces and vertical splitting of specimens parallel to loading

Fig. 11. Failed specimens under cyclic tests.

direction. Because of less difference in strengths and elastic properties of coarse aggregate and mortar. A very few failure planes were observed as compared to normal concrete since, the concrete is of high strength and number of potential failure planes are less.

The amount of bond cracks was also less because of the compatibility between the strength and elastic properties and also higher tensile bond strength. Hence, it can be said that the behavior of High strength GPC is more homogenous than that of normal strength concrete, leading to a smooth and vertical failure plane. After a potential failure plane is developed, it grows in nearly flat plane causing failure. It was also observed that failure was sudden with very few micro-cracks. Fig. 11 shows the failed specimens of GPC.

4.5. Plastic strain variation

"Plastic strains can be defined as strains corresponding to a zero-stress level on the loading or unloading stress-strain curve". For perfectly homogenous materials like structural steel, the loading-unloading curve can coincide with one another and also, they are parallel to initial loading curves. However, this is not the same case for concretes as many researchers are of the view that curves do not coincide and are not parallel and they change with loading histories.

It can be inferred that the plastic strains in the concrete signify the damage of materials and may be connected to the permissible stress levels. Thus, it becomes necessary to relate the plastic strain

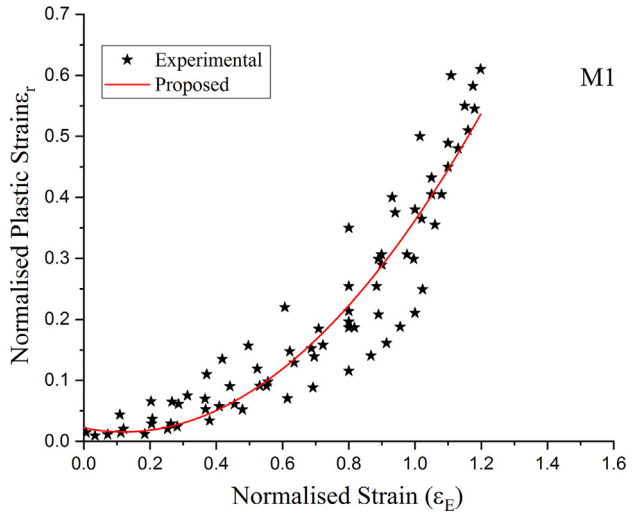

Fig. 12a. Plastic strain Vs Envelope Strain for M1 Mix.

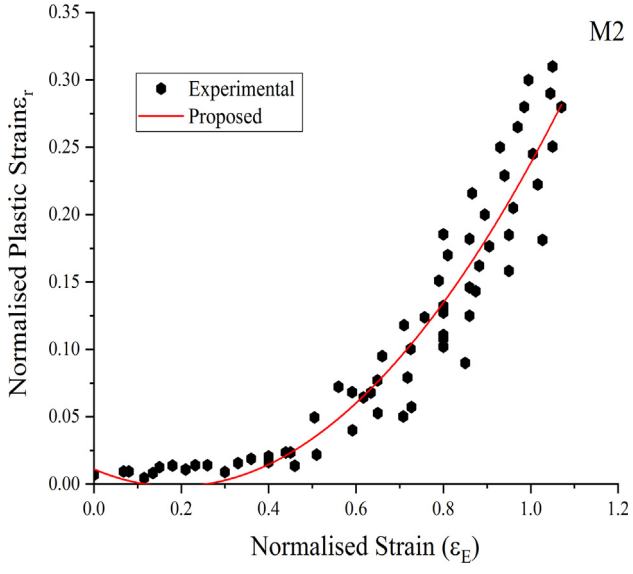

Fig. 12b. Plastic strain Vs Envelope Strain for M2 Mix.

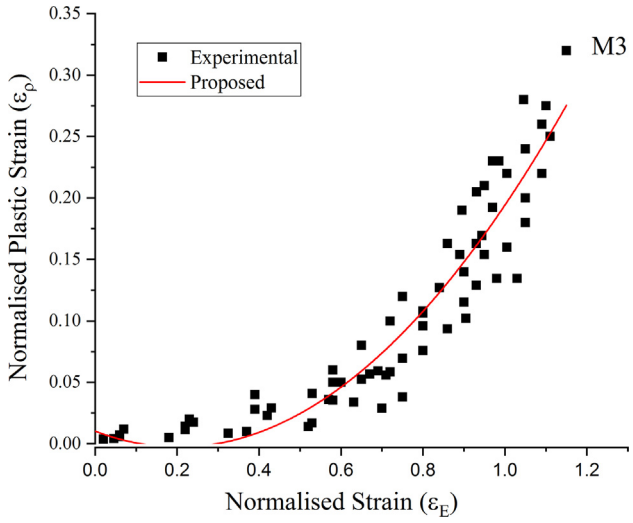

Fig. 12c. Plastic strain Vs Envelope Strain for M3 Mix.

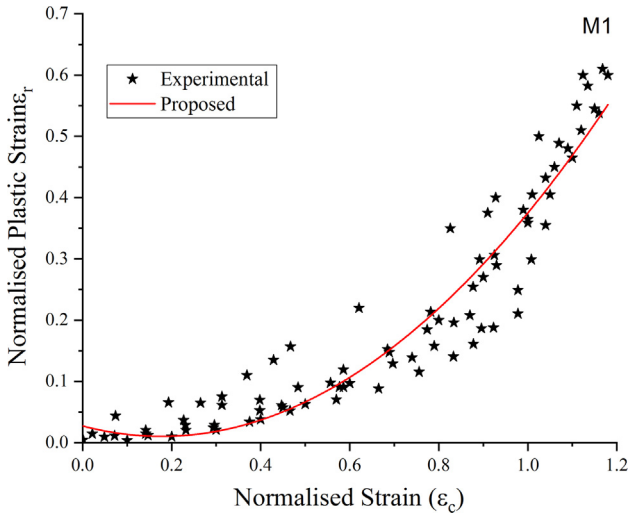

Fig. 13a. Plastic strain Vs Common point for M1 Mix.

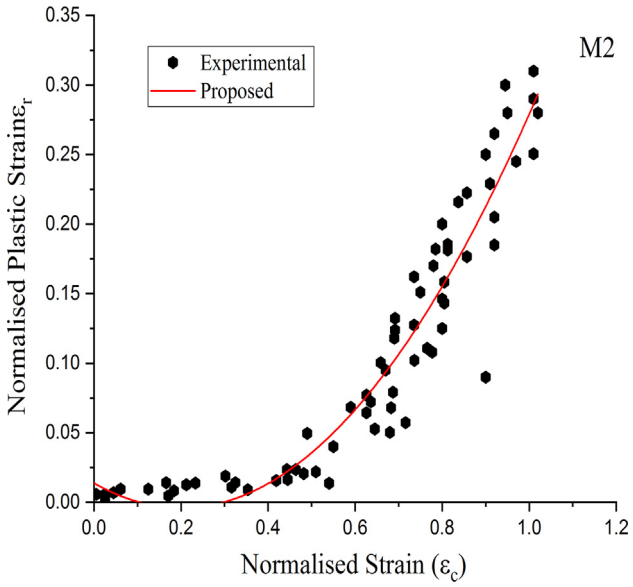

Fig. 13b. Plastic strain Vs Common point for M2 Mix.

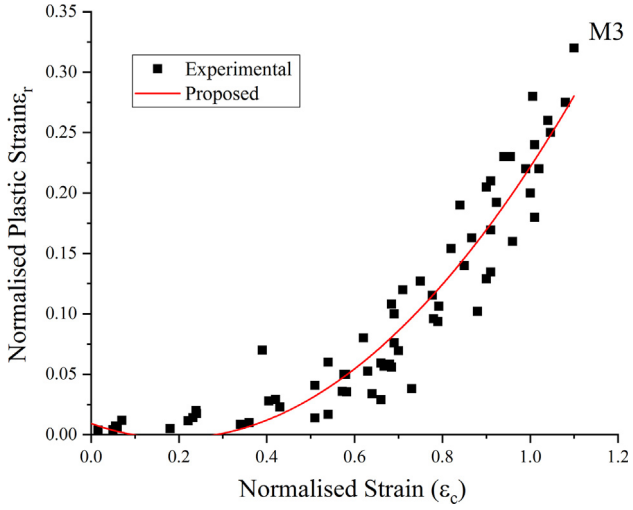

Fig. 13c. Plastic strain Vs Common point for M3 Mix.

to common point, stability point and envelope strain. The mean slope of the loadings and unloading curves are inversely proportional to plastic strain ratio. Loading curve at small plastic strain consists of approximately constant slope till their corresponding limit. When it exceeds the shakedown stresses, plastic strains accelerate to form curves with a reducing slope. The microcracks formed in the material due to loading causes the change in slope. However, when plastic strain ratio is large, loading curve has a point of inflection in stress-strain curves.

Fig. 12a–c shows plastic strain as a function of envelope strain at unloading for all the 3 mixes i.e. M1, M2 and M3. As discussed earlier, the changes in the stress-strain curve with increase or decrease in plastic strain implies that there is a relation between plastic strain ratio and nature of loading curve and un-loading curve. It can be observed from Fig. 12a–c that when the points are combined to form a curve, it shows a general relation between residual strains and un-loading strains. Plastic strains are non-dimensionalized regarding strains when peak loads are attained for all specimens.

Plastic as well as envelope strain is normalized pertaining to e_m, i.e. strain at peak stresses. Figs. 13a–c and 14a–c shows the curves of non-dimensional plastic strains at unloading versus the non-dimensional common point and stability strain respectively.

From the experimental data, variations of plastic strains versus envelope strains, common point strains and stability point strains can be expressed by-

$$\varepsilon_r = C + B_1\varepsilon + B_2\varepsilon^2 \quad (2)$$

where,

ε_r = Normalized plastic-strain;
ε = Normalized strain at envelope, ε_E, common-point, ε_c or stability-point, ε_s;
B_1, B_2 = equation parameter.

Equation parameters, i.e. B_1 and B_2 can be calculated by analyzing the experimental data and for all the mixes M1, M2 and M3 are given in Table 5. It can be observed that the correlation index I_c for all the 3 mixes are above 0.9 indicating a good correlation between experimental data and analytical curve.

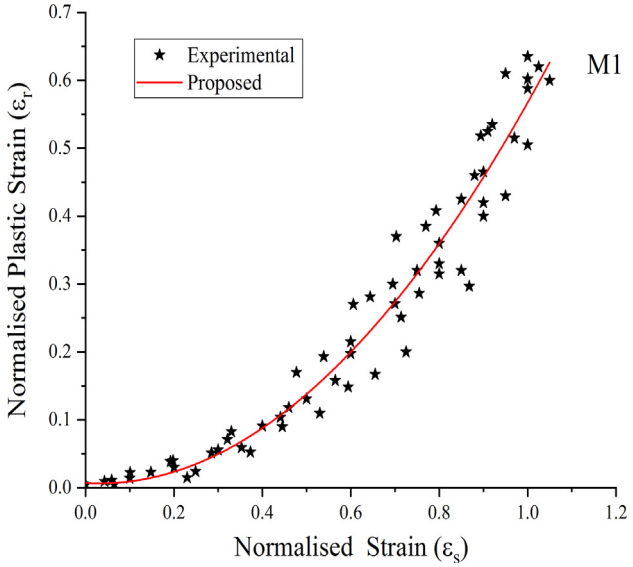

Fig. 14a. Plastic strain Vs Stability point for M1 Mix.

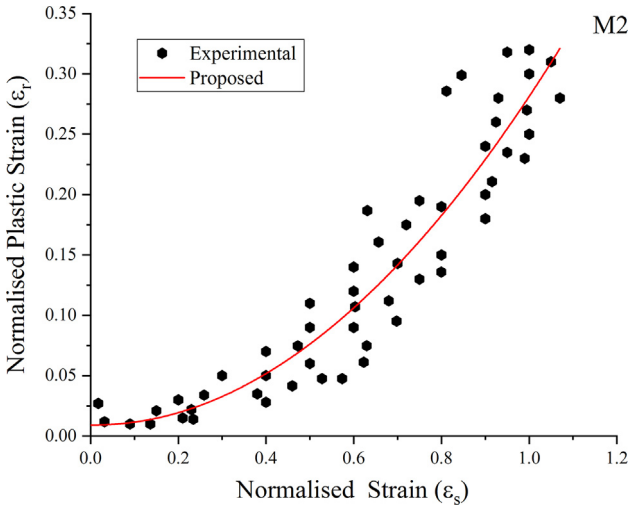

Fig. 14b. Plastic strain Vs Stability point for M2 Mix.

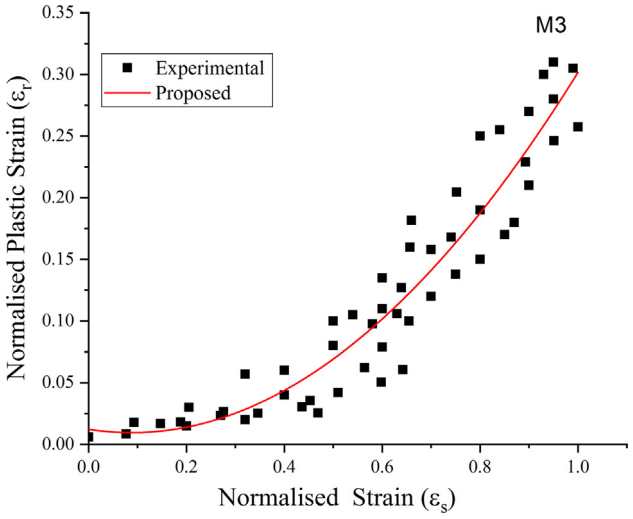

Fig. 14c. Plastic strain Vs Stability point for M3 Mix.

Table 5
Equation parameters and correlation index.

Curve	M1			
	B1	B2	C	I_c
ε_r vs. ε_E	−0.10	0.44	0.022	0.94
ε_r vs. ε_c	−0.19	0.53	0.027	0.93
ε_r vs. ε_s	−0.03	0.54	0.001	0.95
	M2			
ε_r vs. ε_E	−0.13	0.36	0.011	0.94
ε_r vs. ε_c	−0.17	0.44	0.013	0.93
ε_r vs. ε_s	−0.004	0.27	0.0092	0.95
	M3			
ε_r vs. ε_E	−0.12	0.31	0.010	0.93
ε_r vs. ε_c	−0.13	0.34	0.0093	0.93
ε_r vs. ε_s	−0.061	0.35	0.012	0.95

5. Conclusions

The objectives of the study were to examine the behaviour of high strength GPC under repeated loading and to develop an analytical representation of its cyclic behaviour and to provide infor-

mation useful for design and analysis of concrete structures. An envelope stress-strain curve, a locus of common points and a locus of stability points were obtained from the experimental repeated stress-strain curves. The use of the stability point curve in defining the permissible stress levels of GPC, where reduction of compressive strength due to the effect of repeated loading have to be taken in to account, was discussed.

The envelope curves under cyclic compressive loading coincide with stress-strain curves under monotonic loadings for GPC.

The locus of common and stability points was determined from the cyclic stress-strain curve. The identification of these is an important contribution for the design of GPC.

The nature of non-dimensional form of envelope curves is similar but possess higher stress ratio for the higher strength. The common point limit is the same for all the three grades investigated. The stability point curve for M3 concrete exhibits a higher stress ratio than for M2 and M1 concrete.

The stress-strain stability point curve can be used to define the permissible stress level for GPC structures subjected to repeated loading, where reduction in compressive strength due to the effect of these loads has to be considered.

The mean strain values obtained were 0.00299, 0.003 and 0.0031 with a SD of 1.9×10^{-4}, 6.01×10^{-5} and 5.29×10^{-5} for M40, M50 and M60 mixes.

The mean Stress values obtained were 47.20, 56.98 and 63.63 MPa with a SD of 1.9, 2.8 and 2 MPa for M40, M50 and M60 mixes.

Analytical equations were proposed for envelope curve, common points curve and stability points curve for all the 3 mixes. The Proposed curves fit well with experimental test data.

Thus, the level of plastic strain plays a vital role to determine permissible stress level. Hence, in this study, the peak stress of stability point curve is considered as the maximum permissible stress level of GPC subjected to cyclic loading. This study provides a factor of safety of 1.2, whereas IS code specifies a value of 1.5.

CRediT authorship contribution statement

Aslam Hutagi: Conceptualization, Formal analysis, Investigation. **R.B. Khadiranaikar:** Methodology, Validation, Supervision. **Aijaz Ahmad Zende:** Software, Writing - original draft.

Declaration of Competing Interest

The authors declare that they have no known competing financial interests or personal relationships that could have appeared to influence the work reported in this paper.

Acknowledgement

We would like to kindly acknowledge the use of equipment, scientific and technical assistance in Basaveshwar Engineering College, Bagalkot under TEQIP phase-II. We would like to thank the management of SECAB IET, Vijayapura for supporting us throughout the research work.

References

[1] S.A. Sheikh, S.M. Uzumeri, Strength and ductility of tied concrete columns, J. Struct. Div. ASCE 106 (ST5) (1980) 1079–1102.
[2] J.B. Mander, M.J.N. Priestley, R. Park, Theoretical stress–strain model for confined concrete, J. Struct. Eng. 1148 (1988) 1804–1826.
[3] M. Saatcioglu, S.R. Razvi, Strength and ductility of confined concrete, J. Struct. Eng. 118 (6) (1992) 1590–1607.
[4] J. Hoshikuma, K. Kawashima, K. Nagaya, A.W. Taylor, Stress–strain model for confined reinforced concrete in bridge piers, J. Struct. Eng. 123 (5) (1997) 624–633.
[5] B.P. Sinha, K.H. Gerstle, L.G. Tulin, Stress-strain relations for concrete under cyclic loading, J. Am. Concr. Inst. 612 (1964) 195–211.
[6] I.D. Karsan, J.O. Jirsa, Behavior of concrete under compressive loadings, J. Struct.. Div. ASCE 9512 (1969) 2543–2563.
[7] B.Y. Bahn, C.T. Hsu, Stress-strain behavior of concrete under cyclic loading, ACI Mater. J. 95M18 (1998) 178–193.
[8] R. Park, D.C. Kent, R.A. Sampson, Reinforced concrete member with cyclic loading, J. Struct. Div. ASCE 987 (1972) 1341–1360.
[9] J.B. Mander, M.J.N. Priestley, R. Park, Observed stress–strain behavior of confined concrete, J. Struct. Eng. 1148 (1988) 1827–1849.
[10] L.L. Dodd, N. Cooke, The dynamic behaviour of reinforced-concrete bridge piers subjected to New Zealand seismicity, Res. Rep. 92-04, Dept. of Civil Engineering, Univ. of Canterbury, Christchurch, New Zealand, 1992.
[11] E. Martinez-Rueda, A.S. Elnashai, Confined concrete model under cyclic load, Mater. Struct. 30 (1997) 139–147.
[12] L.L. Mendola, M. Papia, General stress–strain model for concrete or masonry response under uniaxial cyclic compression, Struct. Eng. Mech. 144 (2002) 435–454.
[13] J. Sakai, K. Kawashima, G. Shoji, A stress–strain model for unloading and reloading of concrete confined by tie reinforcement, J. Struct. Mech. Earthquake Eng., Japan Soc. Civil Eng. 654/I-52 (2000) 297–316. in Japanese.
[14] J. Sakai, K. Kawashima, An unloading and reloading stress-strain model for concrete confined by tie reinforcement, 2000.
[15] R.B. Khadiranaikar, S.N. Sinha, High Performance Concrete Under Cyclic Loading, IIT Delhi, 2003 (Ph.D. thesis).
[16] Pradip Nath, Prabir Kumar Sarker, Use of OPC to improve setting and early strength properties of low calcium fly ash geopolymer concrete cured at room temperature, Elsevier Cem. Concr. Compos. 55 (2015) 205–214.
[17] Kunal Kupwade-Patil, N. Erez, P. Allouche, Impact of alkali-silica reaction on fly ash-based geopolymer concrete, ASCE J. Mater. Civil Eng. 25 (1) (2013).
[18] Chaicharn Chotetanorm, Prinya Chindaprasirt, Vanchai Sata, Sumrerng Rukzon, Apha Sathonsaowaphak, High-calcium bottom ash geopolymer: sorptivity, pore size, and resistance to sodium sulfate attack, ASCE J. Mater. Civil Eng. 25 (1) (2013).
[19] Zhang Yunsheng, Sun Wei, Chen Qianli, Chen Lin, Synthesis and heavy metal immobilization behaviour of slag based geopolymer, J. Hazard. Mater. 143 (2007) 206–213.
[20] P. Balaguru, Geopolymer for the protective coating of Transportation Infrastructures, 1998, Final report FHWANJ, 0-12
[21] Partha Sarathi Deb, Pradip Nath, Prabir Kumar Sarkar, The effects of ground granulated blast-furnace slag blending with fly ash and activator content on the workability and strength properties of geopolymer concrete cured at ambient temperature, Elsevier Mater. Des. 62 (2014) 32–39.
[22] Pradip Nath, Prabir Kumar Sarkar, Effect of GGBFS on setting, workability and early strength properties of fly ash geopolymer concrete cured in ambient condition, Elsevier Constr. Build. Mater. 66 (2014) 163–171.
[23] Gaurav Nagalia, Yeonho Park, Ali Abolmaali, Pranesh Aswath, Compressive strength and microstructural properties of fly ash-based geopolymer concrete, J. Mater. Civ. Eng. ASCE (2016).
[24] A. Karthik, K. Sudalaimani, C.T. Vijaya Kumar, Investigation on mechanical properties of fly ash-ground granulated blast furnace slag based self-curing bio-geopolymer concrete, Constr. Build. Mater. 149 (2017) 338–349.
[25] Musaad Zaheer Nazir Khan, Faizuddin Ahmed Shaikh, Yifei Hao, Hong Hao, Synthesis of high strength ambient cured geopolymer composite by using low calcium fly ash, Constr. Build. Mater. 125 (2016) 809–820.
[26] Lateef Assi, Edward Deaver, Mohamed K. El Batanouny, Paul Ziehl, Investigation of the early compressive strength of fly ash-based geopolymer concrete, Constr. Build. Mater. 112 (2016) 807–815.
[27] H. Allen, Effect of Direction Loading on Compressive Strength of Brick Masonry, in: Proc. 3rd Int. Brick Masonry Conference, 1973, pp. 98–105.
[28] Indian standards (IS-516), Methods of tests for strength of concrete, Bureau of Indian Standards, New Delhi, 1959 (Reaffirmed 1999), 25 pp.